Fracture mechanics model for predicting fracture strength of metallic alloys containing large second phase particles

Uwe Zerbst* and Mauro Madia

BAM-Federal Institute for Materials Research and Testing, 9.1
D-12205 Berlin, Germany
* Corresponding author: uwe.zerbst@bam.de

Abstract An analytical fracture mechanics model for predicting the finite life fatigue strength of components is presented which combines a number of well established and newly developed approaches such as Murakami's and McEvily's approach for describing the transient behaviour of crack closure of short cracks, the analytical (long) crack closure function of Newman, the R6 procedure modified by a method for improving the ligament yielding correction proposed by the authors and other elements. Basic assumption is the preexistence of initial flaws such that the crack initiation or nucleation stage is small and can be neglected. The application of the model is demonstrated for small tension plates of aluminium Al 5380 H321 with artificial initial defects generated by FIB technology, the size of which was fixed on the basis of fractographic investigations on broken, smooth specimens.

Keywords fatigue strength, S-N curve, fracture mechanics, crack propagation, short cracks

1. Introduction

The lifetime of a cyclically loaded component can be roughly subdivided into three stages: crack initiation, fatigue crack propagation and fracture. Frequently the crack initiation stage is defined such that it covers nucleation and early crack propagation until the crack reaches some tenth of a millimetre at surface. However, a closer look reveals that this phase can be subdivided in a number of sub-stages (e.g. [1]):

(a) The crack initiation sub-stage in a narrower sense which is characterised by the accumulation of microscopic plastic deformation sometimes occurs at the smooth surface but more frequently it happens at scratches, pores, inclusions and similar defects which act as micro-notches and/or due to strain concentration zones caused by different stiffness properties of defect and matrix material. In the case of very high cycle fatigue (fracture after 10^8 loading cycles or more) initiation takes place subsurface but also at material defects [2].

(b) Subsequent to crack initiation the crack size is in the range of micro-structural features such as the grain size. Its propagation is characterised by a irregular crack front and alternating phases of acceleration and retardation or even crack arrest. The arrest of the largest of a number of initially growing cracks is associated with the fatigue limit phenomenon [3].

(c) With the increasing crack size the effect of the microstructure on local fatigue crack propagation diminishes and the propagation rate becomes rather steady. When the crack size reaches the order of mechanical discontinuities such as the plastic zone size or a notch stress field the crack is designated as mechanically short. Its propagation, in principle, can be described by classical fracture mechanics, however not by the linear elastic ΔK concept. As the micro-structurally short crack also the mechanically short one can be arrested under constant applied loading due to the gradual build-up of the plasticity-induced crack closure phenomenon.

(d) Long cracks propagate above a crack-size independent long-crack threshold ΔK_{th}. Their growth can be described by the da/dN-ΔK curve concept when the crack closure phenomenon is taken into account. The long crack propagation is terminated by the fracture of the component.

The crack initiation sub-stage in the narrower sense frequently is very limited for many engineering materials. Instead of a detailed discussion a statement of Polak in Elsevier's"Comprehensive Structural Integrity" shall be cited here: "Numerous studies have shown that in the majority of materials and under normal loading conditions, the period of crack initiation in smooth specimens without defects amounts to less than 5-20% of the fatigue life. In materials containing defects, the fraction of life spent in crack initiation is even lower. The major part of the life is spent in the growth of cracks, namely in the growth of short cracks." [1]. This fact allows to model metallurgical defects as initial cracks without yielding over-conservative lifetime predictions.

2. Model Proposed for Predicting Finite-life Fatigue Strength and Lifetime

The observation that the essential part of fatigue lifetime of many engineering materials is covered by short crack growth requires a fracture mechanics model which is able to describe this stage in an adequate manner. The authors proposed such a model in [4] where the reader can also find a more detailed description as it is possible here due to limited space. The model, for a number of partial aspects, uses and combines otherwise established approaches because of which there exist similarities with alternative models (e.g. [5-8]) which also cannot be discussed here in any detail. Instead, the reader is referred to [4]. Fig. 1 summarises the input and model parameters and the analysis steps of the present procedure. In the following the analysis steps shall be exemplarily explained for tension plates of aluminium alloy Al 5083 H 321. This will then be added by validation exercises on two more aluminium alloys the data of which were taken from the literature.

2.1 Initial crack size

For the present study fracture surfaces of cyclically tension loaded flat plates were fractographically analysed. A fracture surface containing an initial defect is shown along with a micrograph section and statistics of the defect sizes found on all specimens in Fig. 2. In Fig. 2(d), following a proposal of Murakami (e.g. [2]), the initial crack size is given as the square root of its area, $\sqrt{\text{area}}$, with the index "i" standing for "initiation". The statistical upper bound of the initial defect depth was found to be in the order of 50 μm which is quite typical for aluminium alloys [9].

2.2 Material properties

The material properties needed as input parameters of the proposed model comprise the da/dN-ΔK curve for the stress ratio $R = K_{min}/K_{max}$ of interest (in the present case R = 0.2), the long crack fatigue threshold ΔK_{th} for the same R, the intrinsic threshold (no plasticity-induced crack closure) and the stabilised cyclic stress-strain curve. The Paris range of the da/dN-ΔK curve was experimenttally determined for R = 0.2 on four specimens. The average value of C was C = $4.05 \cdot 10^{-12}$ (ΔK in $\text{MPa}\sqrt{\text{mm}}$; da/dN in mm/loading cycle) for an n assumed as n = 3. The threshold values for R = 0,2 und R $\rightarrow$ 1 (intrinsic value) were 1.5 $\text{MPa}\sqrt{\text{m}}$ and 0.925 $\text{MPa}\sqrt{\text{m}}$ respectively.

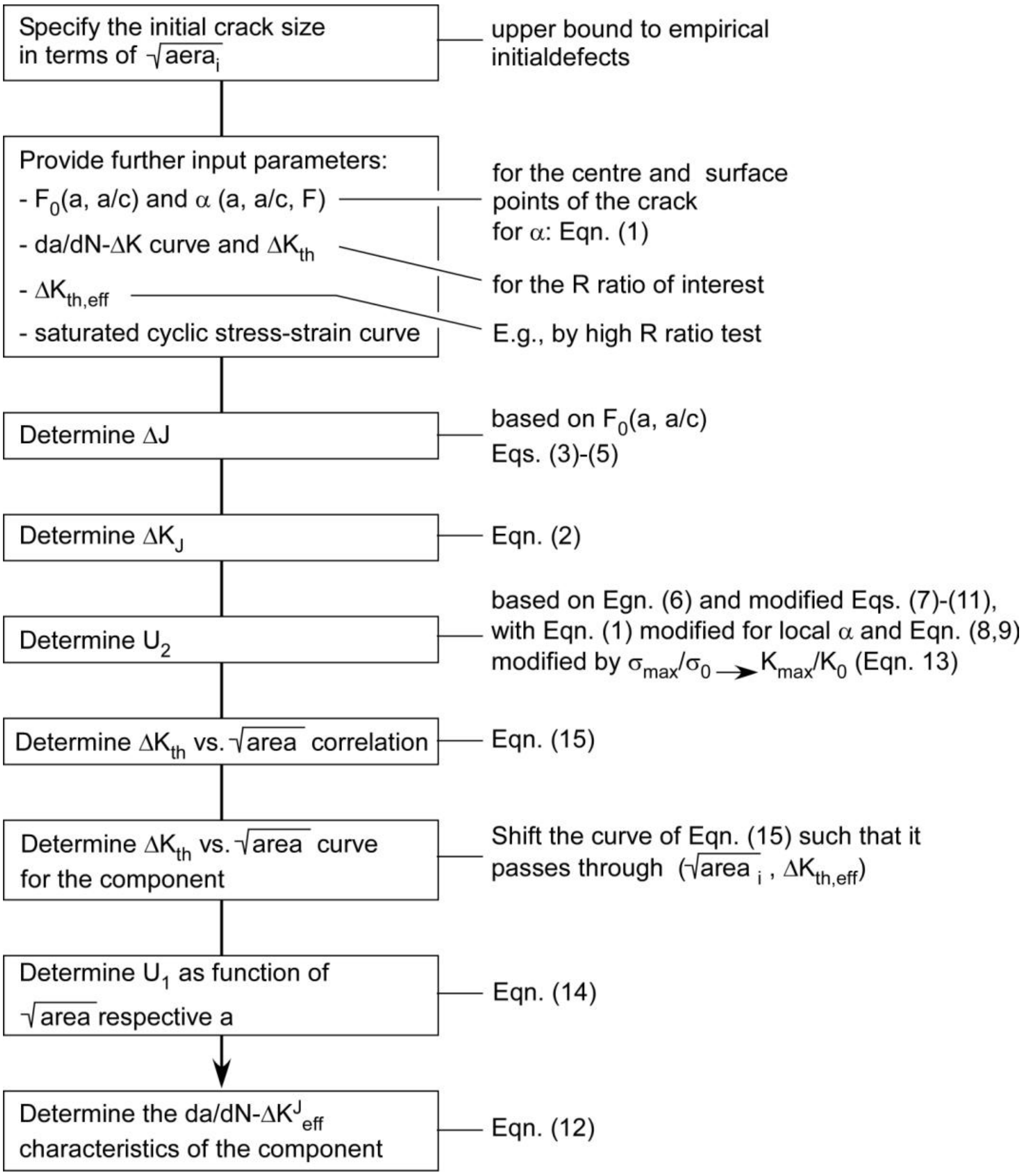

Fig. 1: Input and model parameters and steps of the fracture mechanics model presented here.

2.3 Model parameters

The model parameters of the analysis are the linear elastic stress intensity factor K for the deepest and the surface points at the crack front which were obtained by the solution of Raju and Newman [10] and confirmed by finite elements.

Following a proposal of the authors in [11] the reference load F_0 replaces the limit load in assessment procedures such as R6 [12] or SINTAP [13]. It is defined as that load at which the ligament plastification $L_r = F/F_0 = 1$. This may be different for different positions at the crack front.

A local constraint parameter α was determined instead of the global value according to Newman [14] the latter being given by Eqn. (1):

$$\alpha_g = \frac{1}{A_T} \sum_{m=1}^{M} \left(\frac{\sigma_{yy}}{\sigma_0} \right)_m A_m \qquad (1)$$

(A_m = projected area of a yielded element m on the uncracked ligament, σ_{yy}/σ_0 = normalized crack opening stress for the element m, A_T = total projected area of all elements (M) which have yielded)

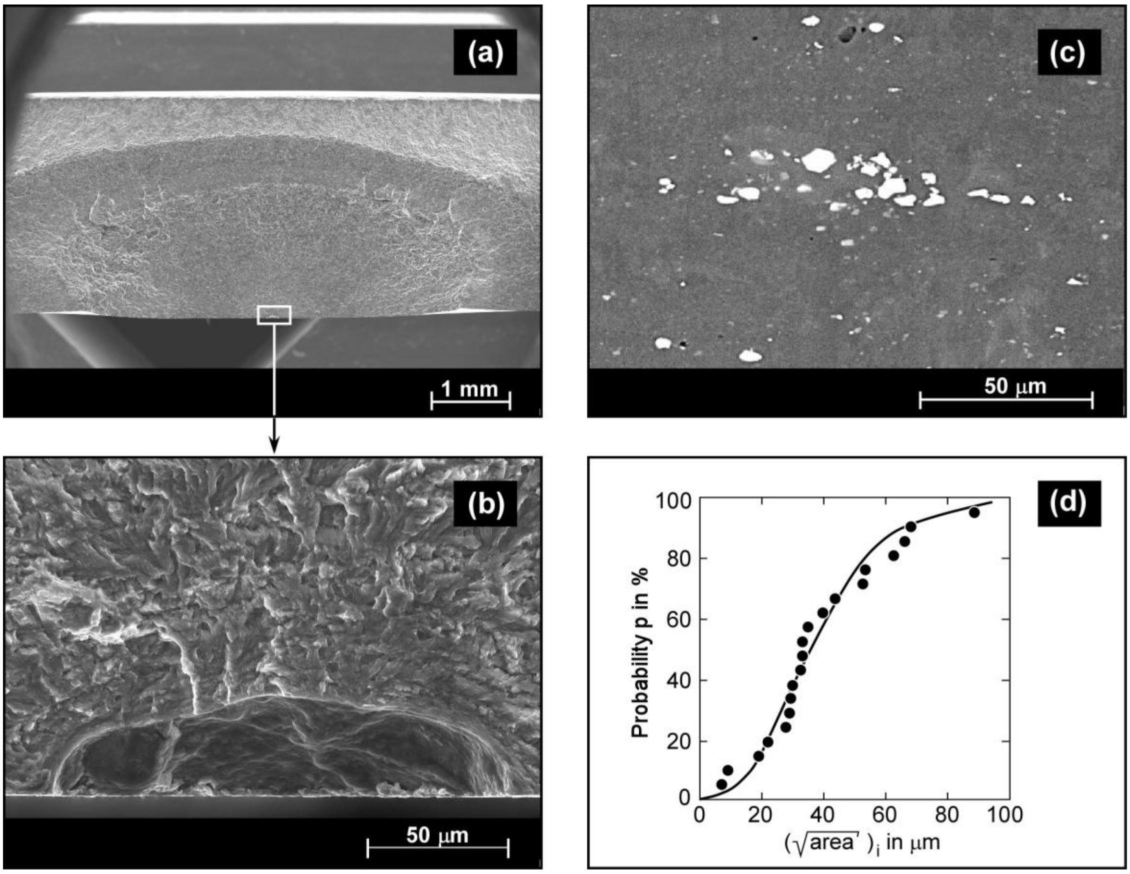

Fig. 2: Initial defects in the material AL5380 H321, fractographic and metallographic investigations: (a) and (b) example for an initial defect; (c) a cluster of inclusions with increased concentration of manganese, iron and nickel; (d) statistical distribution of the initial crack depth.

The parameter has been obtained by finite elements as a local parameter separately for the deepest and surface points of the semi-elliptical surface crack by modifying Eqn. (1) such that the total area of the plastic zone ahead of the crack, A_T, is replaced by local areas around the two points of interest. A more detailed description of the concrete realisation is found in [15].

2.4 Crack driving force of mechanically short cracks

The considerations in this paper mainly focus on short crack propagation (see Section 1). This is no problem insofar as the maximum initial defect sizes found at the fracture surfaces (see Fig. 2d) were sufficiently large not to be micro-structurally short cracks any more. It has already been mentioned that mechanically short cracks cannot adequately been described by the ΔK concept since the size of the plastic zone ahead of the crack is in the same order as the crack length. In order to address the local yielding effect ΔK is replaced by a ΔK^J which is formally obtained as

$$\Delta K^{J} = \sqrt{\Delta J \cdot E'}$$
$$E' = \begin{cases} E & \text{plane stress} \\ E/\ 1-\nu^2 & \text{plane strain} \end{cases} \tag{2}$$

With respect to a discussion of the cyclic J integral, ΔJ, the reader is referred to [4]. Within this paper a (slightly modified) approach of McClung [16,17] is applied by which ΔJ is determined by

$$\Delta J = \frac{\Delta K^2}{E'} \cdot \left[f \quad \Delta L_r \quad \right]^{-2} \tag{3}$$

with $$\Delta L_r = \frac{\Delta F}{2F_Y} = \frac{\Delta\sigma_{ref}}{2\sigma_Y}\,. \tag{4}$$

and $$L_r = F/F_0\,. \tag{5}$$

2.5 Modelling the plasticity-induced crack closure pheneomenon

With respect to modelling the crack closure effect it has to be distinguished between long cracks (the effect is completely build-up) and short cracks (the effect is still gradually developing). Crack closure is described by a parameter U (U_1 – short crack; U_2 – long crack). For the long crack the so-called NASGRO equation is used which is based on results obtained by applying the modified strip yield model of Newman [18]:

$$U_2 = \frac{\Delta K_{eff}}{\Delta K} = \frac{1-f}{1-R} \tag{6}$$

$$\text{with} \quad f = \frac{\sigma_{open}}{\sigma_{max}} = \begin{cases} A_0 + A_1R + A_2R^2 + A_3R^3 & \text{for } R \geq 0 \\ A_0 + A_1R & \text{for -2<}R < 0 \end{cases} \tag{7}$$

The coefficients A_i are given by

$$A_0 = \ 0.825 - 0.34\alpha_g + 0.05\alpha_g^2 \ \left[\cos\left(\frac{\pi/2 \cdot \sigma_{max}}{\sigma_0} \right) \right]^{1/\alpha_g} \tag{8}$$

$$A_1 = \ 0.415 - 0.071\alpha_g \ \frac{\sigma_{max}}{\sigma_0} \tag{9}$$

$$A_2 = 1 - A_0 - A_1 - A_3 \tag{10}$$

$$A_3 = 2A_0 + A_1 - 1 \tag{11}$$

For the present model Eqs. (8) to (11) have been modified in several aspects:

(a) The ΔK parameter is replaced by ΔK^J. The determination of the parameter is as described above. The complete modified crack propagation equation is then:

$$\frac{da}{dN} = C\left(\Delta K^J_{eff}\right)^n = C\begin{cases}\left(U_1 \Delta K^J\right)^n & a_i < a < a^* \\ \left(U_2 \Delta K^J\right)^n & a_i \geq a^*\end{cases} \tag{12}$$

(b) Originally the f function in Eqn. (7) has been obtained for centre-cracked plates subjected to uniform tension. The question arises whether it can also be applied to other configurations, for example bending geometries. McClung at al. [19] (see also [17]) carried out extended finite element investigations on M(T) center-cracked plates in tension, SE(T) single-edge-cracked plates in tension, SE(B) single-edge-cracked plates in bending and pure bending geometries and concluded that the f-function and, as a consequence, the crack opening stress σ_{open} (or K_{op}) are more accurately correlated by the K_{max}/K_0 ratio than by σ_{max}/σ_0 in Eqs. (8) and (9). They proposed to substitute the latter by K_{max}/K_0:

$$\frac{K_{max}}{K_0} = \frac{Y\sigma_{max}\sqrt{\pi a}}{\sigma_0\sqrt{\pi a}} \tag{13}$$

Other authors [20,21] have also found K_{max}/K_0 to be a superior parameter. Therefore, it is adopted in the present study too.

(c) The constraint parameter α in Eqs. (8) and (9) is not used as a fixed parameter as in the NASGRO approach but determined by finite element analyses based on Eqn. (1), but determined as local parameter for points A and C of the crack.

(d) The reference stress σ_0 in Eqs. (8), (9) and (13) is not chosen as the average of the quasi-static yield and tensile strength as in NASGRO but as the cyclic yield strength.

With respect to the gradual build-up of the plasticity-induced crack closure effect for the short crack stage the model assumes that the latter is mirrored in the development of the short crack fatigue threshold (as e.g. in [6]). The parameter U_1 can then be determined by

$$U_1 = \frac{U_2}{\Delta K_{th}(a)/\Delta K_{th,lc}} \tag{14}$$

with the index „lc" designating the long crack. The ΔK_{th}-crack depth function is described by an approach of McEvily et al. [22]

$$\Delta K_{th} = \Delta K_{op} + \Delta K_{th,eff} = \left[1 - e^{-k\cdot(a-a_0)}\right]\cdot \Delta K_{op,max} + \Delta K_{th,eff} \tag{15}$$

but modified by replacing the crack depth a by an equivalent crack depth $\sqrt{area}$ as introduced above. In Eqn. (15) k is a fit parameter which describes how the crack closure effect develops as a function of a-a_0 or $\sqrt{area} - \sqrt{area_0}$ respectively. Since Eqn. (15) includes two fit parameters, k and a_0

or $\sqrt{area_0}$, a minimum of two conditional equations is necessary. The first one is $\Delta K_{th} = 0$ für $\sqrt{area} = 0$; the second on is given by $\Delta K_{th} \propto \sqrt{area}^{\,1/3}$ for an arbitrary crack size. For steels, according to [2], this can be realised by an estimate

$$\Delta K_{th} = 3{,}3 \cdot 10^{-3} \left(HV + 120 \right) \Big/ \left(\sqrt{area} \right)^{1/3} \tag{16}$$

with HV being the Vickers hardness. However, for the aluminium alloy investigated in this study no similar solution exists. Therefore, an alternative solution had to be found which will be described in Section 3.

As assumed in [22] the threshold ΔK_{th} is subdivided into an intrinsic value, $\Delta K_{th,eff}$, and an additional amount due to the crack closure effect, $\Delta K_{th,op}$. The intrinsic term is a lower bound which exists even if no crack closure effect occurs (therefore the designation “eff”). It can, e.g., be determined by experiments at different R ratios and extrapolation for R → 1 as realised in the present paper. Because the state of the initial defect is characterised by both, the intrinsic threshold $\Delta K_{th,eff}$ and the initial crack area (respective its square root $\left(\sqrt{area}\right)_i$ the curve according to Eqn. (15) has to be shifted to pass through this point such as shown in Figure 3. The prediction of the ΔK_{th} versus crack size curve in the component is then provided by the un-dotted dark line. The transition between short and long crack propagation occurs at $\sqrt{area}^{\,*}$, where the ΔK_{th} according to the (shifted) Eqn. (15) curve intersects the long crack threshold value.

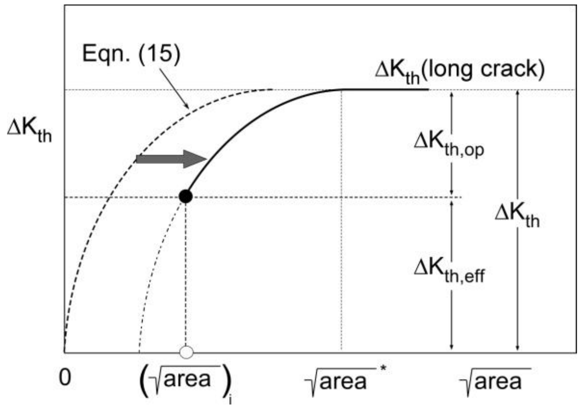

Fig. 3: Proposed method for determining the ΔK_{th}-crack size correlation for short cracks in the present model.

3. Validation on AL5380 H321 specimens

The validation of the model was performed with specimens prepared with artificial initial defects. Using the FIB (Focus Ion Beam) technology notches with a notch width of 6 μm, a depth of a = 37.4 μm and a length at surface 2c = 101.25 μm were generated.[1)]

[1)] The authors wish to thank Dr. Erica Lilleodden, HZG Geesthacht, who prepared the FIB cracks.

The notch dimensions were identical for all validation specimens. With an area of 3230 μm^2 or $\sqrt{area}_i \approx 57\ \mu m$ the size of these artificial defects referred to the upper tail of the statistical distribution of the natural defects found on the fracture surfaces as shown in Fig. 2(d). The prepared specimens were then used to generate an S-N curve. The tests were interrupted when cracks of about 2c = 3 mm were visible at the specimen surfaces. The stress-strain data of the material were: cyclic proof strength $R_{p0.2,cyc}$ = 341 MPa and cyclic modulus of elasticity E_{cyc} = 68.4 GPa.

It has already been mentioned in Section 2.5 that Eqn. (16) was not applicable to the aluminium alloy investigated. Therefore, an alternative second conditional equation had to be used. This is given by a general form

$$\Delta K_{th} = 3.3 \cdot 10^{-3} C_0 \left(\sqrt{area}\right)^{1/3} \tag{17}$$

with $\sqrt{area}_i$ referring to the size of the artificial initial defect and C_0 being a material constant which, according to Murakami [2], correlates with the fatigue limit σ_e (in the present case the fatigue strength at 10^7 loading cycles) by

$$C_0 = \frac{1}{1.43} \sigma_e \left(\sqrt{area}\right)^{1/6}. \tag{18}$$

with σ_e = 80 MPa and $\sqrt{area}_i$ = 56.85 the parameters in Eqn. (15) have finally been determined as $\sqrt{area}_0$ = 20.86 μm, k = 0.0652 μm^{-1} and $\sqrt{area}^*$ = 140 μm. As mentioned above Eqn. (15) curve had to be shifted such that it passed through the point ($\sqrt{area}_i$, $\Delta K_{th,eff}$). This is realised in Fig. 4.

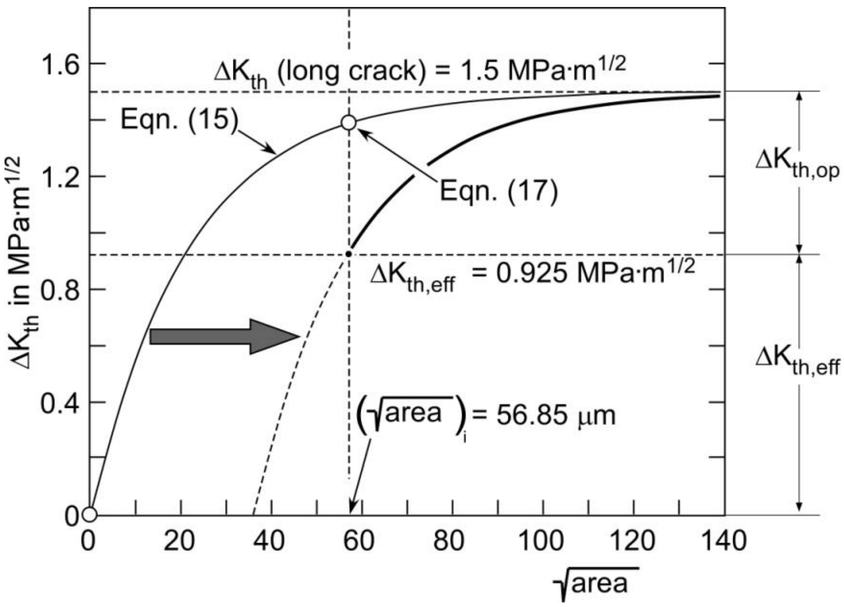

Fig. 4: Application of the model of Figure 3 to the present example.

As the final result the fatigue strength for finite life was predicted as shown in Fig. 5. The analyses were performed for each individual specimen. In addition the predicted and experimental values of the crack size, a and 2c, at test end, are compared in Fig. 5. It shows up that all experimental data were predicted with satisfying accuracy.

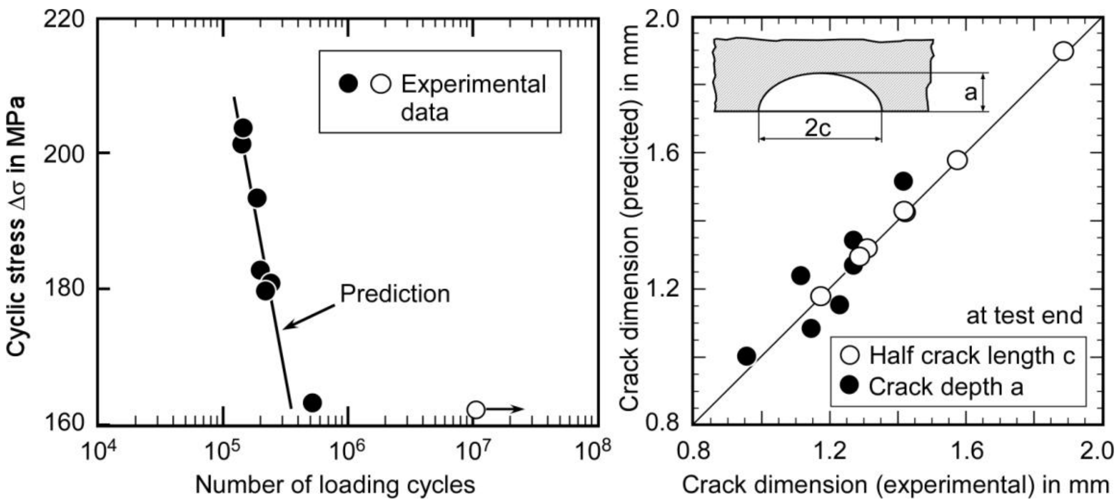

Fig. 5: S-N curve obtained for the tensile plates with artificial (FIB) cracks. Comparison between the experiments and the predictions with the present model.

4. Validation on further aluminium alloys (literature data)

Further validation of the model has been conducted using short crack propagation data from the literature which are available for aluminum alloys commonly used in the aerospace field. In particular, two different alloys have been considered: Al 2024-T3 and Al 7075-T6. An extensive collection of data for these materials is provided in [23] and [24]. Figure 6 shows the S-N lines used for validation. In case of the Al 2024-T3, experimental test data were available for two different load ratios (R = 0, -1) whereas the Al 7075-T6 has been tested at R = 0 only. The specimens did show almost no stress concentration which allowed the use the stress intensity factor and reference load equations already applied to the validation example of section 3. Since no finite element calculations have been conducted for the constraint factor α, such as above, Schijve's equation [25]

$$U = 0.55 + 0.33 \cdot R + 0.12 \cdot R^2 \tag{19}$$

has been used to determine the effective stress intensity factor range for long cracks.

The analytical simulation for the Al 2024-T3 has been performed for a suggested initial crack size of a_i = 20 μm, which resulted from an approximation of the experimental S-N data for both R = 0 and -1. In case of the Al 7075-T6, two different crack sizes have been employed in order to show the impact of a different starting crack size on the calculated number of cycles to failure. Figure 6b shows slightly conservative results a_i = 20 μm which were, however, improved when fractographic data of a_i = 6 μm were used. All simulations have been stopped when the crack reached a final depth of 80% the plate thickness.

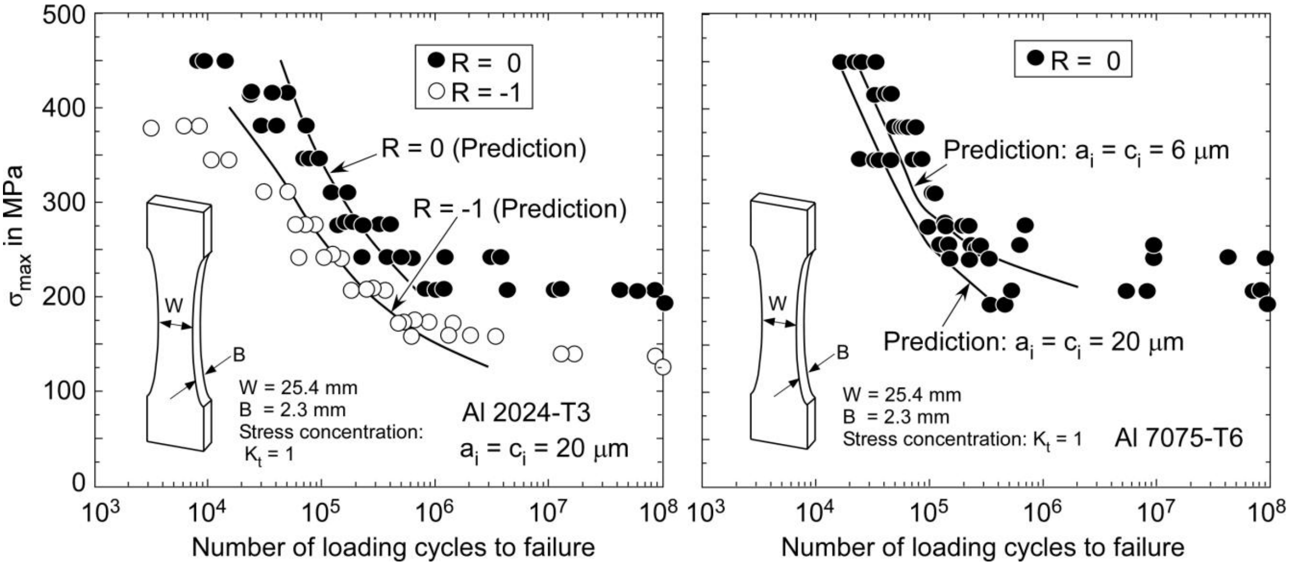

Fig. 6: S-N curves obtained for the tensile plates of two aluminium alloys compared with predictions based on the present model. S-N data taken from [23,24].

5. Summary and Outlook

An analytical fracture mechanics model for predicting the finite life fatigue strength range of the S-N curve was developed. Its application was demonstrated for tension loaded small plates made of different aluminium alloys. The results were promising.

The model is based on a number of assumptions:

(a) In engineering materials fatigue crack propagation initiates at pre-existing material defects such as welding flaws, pores, inclusions etc.

(b) The crack initiation sub-stage in a narrower sense during which a crack develops from the pre-existent defect is typically rather limited. Therefore, a fracture mechanics based lifetime prediction (which per definition is a residual lifetime prediction) yields conservative but not over-pessimistic lifetimes. Note, however, that this has not to be the case for any material.

(c) The initial crack size has been determined by fractographic investigation of fracture surfaces of cyclically loaded specimens.

(d) Since the major part of lifetime belongs to short crack propagation specific issues such as the transient behaviour of crack closure of short cracks and local ligament plasticity effects had to be taken into account.

(e) The presented model is limited to the propagation of mechanically short cracks and not applicable to micro-structurally short ones.

(f) Fracture mechanics based determination of fatigue strength provided significant potential as compared to and in addition to classical fatigue strength concepts because it takes parameters such as weld geometry, residual stresses etc. explicitly into account.

6. References

[1] Polak, J. (2003): Cyclic deformation, crack initiation, and low-cycle fatigue. In: Ritchie, R.O. and Murakami, Y. (Eds.): Comprehensive Structural Integrity; Volume 4: Cyclic loading and Fracture; Elsevier, 1-39.

[2] Murakami, Y. (2003): High and ultrahigh cycle fatigue. In: Ritchie, R.O. and Murakami, Y. (Eds.): Comprehensive Structural Integrity; Volume 4: Cyclic loading and Fracture; Elsevier, 41-76.

[3] Miller, K.J. and O'Donnel, W.J. (1999): The fatigue limit and its elimination. Fatigue & Fracture of Engng. Mater. & Struct. 22, 545-557.

[4] Zerbst, U., Madia, M. und Hellmann, D. (2011): An analytical fracture mechanics model for estimation of S-N curves of metallic alloys containing large second particles. Engng. Fracture Mech. 82, 115-134.

[5] Ishihara, S. and McEvily, A.J. (2002): Analysis of short crack growth in cast aluminium alloys. Int. J. Fatigue 24, 1169-1174.

[6] Bruzzi, M.S. and McHugh, P.E. (2002): Methodology for modelling the small crack fatigue gehaviour of aluminium alloy. Int. J. Fatigue 24, 1071-1078.

[7] McClung, R.C., Chell, G.G., Lee, Y.-D., Russel, D.A. und Orient, G.E. (1997): A practical methodology for elastic-plastic fatigue crack growth. ASTM STP 1296, 317-337.

[8] Eufinger, J., Heinrietz, A., Bruder, T. und Hanselka, H. (2010): Bruchmechanisch basierte Schwingfestigkeitsanalyse von Gusseisen unter Berücksichtigung der Gefügeeigenschaften. 43. Tagung des DVM-Arbeitskreises "Bruchvorgänge, DVM-Bericht 243, 203-213.

[9] White, P. (2006): Review of methods and approaches for the structural risk assessment of aircraft. Australian Defence Science and Technology Organisation, Victoria, Australia, http://www.dtic.mil/cgi-bin/GetTRDoc?Location=U2&doc=
GetTRDoc.pdf&AD=ADA462955

[10] Raju, I.S. and Newman, J.C., Hr. (1979): Stress-intensity factors for a wide range of semi-elliptical surface cracks in finite-thickness plates. Engng,. Fracture Mech. 11, 817-829.

[11] Zerbst, U., Ainsworth, R.A. und Madia, M. (2011): Reference load versus limit load in engineering flaw assessment: A proposal for a hybrid analysis option. Engng. Fracture Mech., upcoming.

[12] R6, Revision 4 (2009): Assessment of the Integrity of Structures Containing Defects. British Energy Generation Ltd (BEGL), Barnwood, Gloucester.

[13] Zerbst, U., Schödel, M., Webster, S. and Ainsworth, R.A. (2007): Fitness-for-Service Fracture Assessment of Structures Containing Cracks. A Workbook based on the European SINTAP/FITNET Procedure. Elsevier.

[14] Newman, J.C., Jr. (1984): A crack opening stress equation for fatigue crack growth. Int. J. Fracture 24, R131-R135.

[15] Beretta S., Carboni, M. and Madia, M. (2006): Fatigue Strength in Presence of Inhomogeneities: Influence of Constraint. Journal of ASTM International. Vol. 3, No. 4.

[16] McClung, R.C., Chell, G.G., Lee, Y.-D., Russel, D.A. und Orient, G.E. (1997): A practical methodology for elastic-plastic fatigue crack growth. ASTM STP 1296, 317-337.

[17] McClung, R.C., Chell, G.G., Lee, Y.-D., Russell, D.A. and Orient, G.E. (1999): Development of a practical methodology for elastic-plastic and fully plastic fatigue crack growth. NASA Report NASA/CR-1999-209428.

[18] Newman, J.C., Jr. (1984): A crack opening stress Equation for fatigue crack growth. Int. J. Fracture 24, R131-R135.

[19] McClung, R.C (1994): Finite element analysis of specimen geometry effects on fatigue crack closure. Fatigue Fracture Engng. Mat. Struct. 17, 861-872.

[20] Liu, J.Z. and Wu, X.R. (1997): Study of fatigue crack closure behaviour for various cracked geometries. Engng. Fracture Mech. 57, 475-491.

[21] Kim, J.H. and Lee, S.B. (2000): Fatigue crack opening stress based on the strip-yield model. Theor. Appl. Fracture Mech. 34, 73-84.

[22] McEvily, A.J., Endo, M. and Murakami, Y. (2003): On the $\sqrt{\text{area}}$ relationship and the short fatigue crack threshold. Fatigue Fracture Engng. Mat. Struct. 26, 269-278.

[23] Newman, J.C., Jr., Phillips, E.P. and Swain, M.H. (1999): Fatigue-life prediction methodology using small-crack theory. International Journal of Fatigue 21, 109-119.

[24] Edwards, P.R. and Newman, J.C., Jr. (1990): AGARD-R-767: Short-crack behaviour in various aircraft materials. AGARD.

[25] J. Schijve, J. (2001): Fatigue of Structures and Materials. Kluwer Academic Publishers. Dordrecht.